Desalination and Water Treatment
www.deswater.com

doi: 10.5004/dwt.2023.29593

295 (2023) 142–149
May

Combination of chemical methods for obtaining ZnO films for application and reuse in photocatalysis: polymeric precursor and microwave-assisted hydrothermal methods

Graziela de Souza[a], João Otávio Donizette Malafatti[b], Jeferson Almeida Dias[c], Elaine Cristina Paris[b], Rodolfo Foster Klein-Gunnewiek[d], Tania Regina Giraldi[a,*]

[a]*Federal University of Alfenas (UNIFAL), Rodovia José Aurélio Vilela, No. 11,999, Poços de Caldas, MG, 37715-400, Brazil, emails: tania.giraldi@unifal-mg.edu.br (R. Giraldi), graziesouza@yahoo.com.br (G. de Souza)*
[b]*Nanotechnology National Laboratory for Agriculture (LNNA), Embrapa Instrumentação Agropecuária, Rua XV de Novembro, 1452, São Carlos, SP, 13560-970, Brazil, emails: jmalafatti@hotmail.com (J.O.D. Malafatti), elaine.paris@embrapa.br (E.C. Paris)*
[c]*Instituto de Ciência, Tecnologia e Inovação (ICTIN), Federal University of Lavras (UFLA), Aquenta Sol, Lavras, MG, 37200-900, Brazil, email: jefersondias@ufla.br (J.A. Dias)*
[d]*Federal University of São Carlos, Rodovia Washington Luís, km 235, São Carlos, SP, 13565-905, Brazil, email: rodolfo.gunnewiek@gmail.com (R.-F. Klein-Gunnewiek)*

Received 22 October 2022; Accepted 22 April 2023

ABSTRACT

This paper evaluated the photocatalytic activity and reuse potential of ZnO films obtained by combining two chemical methods, polymeric precursor (PP) synthesis and microwave-assisted hydrothermal (HMW) synthesis, to remove Rhodamine B dye. This strategy is a promising route to photocatalyst synthesis, allowing easy control of deposition parameters and fast reactions. ZnO films had a hexagonal wurtzite structure and a typical bandgap of 3.3 eV, lower than that of the PP layer (3.9 eV). Films obtained by the PP method showed homogeneous structure and nanometric grain size (32 nm). The use of PP films as a seed layer for particle deposition by the HMW method resulted in films composed of spherical particles (25–137 nm) with an irregular surface. Films obtained after 10 min of PP-HMW reaction showed a less filled surface than those obtained after 30 min of reaction. The kinetic constant increased from 7×10^{-3} min^{-1} by the PP method to 9×10^{-3} min^{-1} by the HMW method. ZnO films obtained by the PP-HMW route had the best photocatalytic performance, achieving 67% dye degradation after 120 min of reaction. This result can be attributed to the presence of an interface between PP and HMW layers, which increases surface irregularity, consequently increasing contact between dye and semiconductor particles. The photocatalyst showed good reusability, achieving 56% dye degradation after five reuse cycles. These findings demonstrate the potential of combining PP and HMW methods to improve the photocatalytic activity of ZnO thin films.

Keywords: Film; Microwave-assisted hydrothermal method; Photocatalyst; Polymeric precursor; ZnO

1. Introduction

Nanomaterials are an important tool for environmental remediation of pollutants [1,2]. ZnO is one of the most important functional oxides with electronic and eco-friendly properties. ZnO materials have been studied for application as sensors [3], varistors [4], antimicrobials [5], fertilizers [6], and catalysts [7]. Given its chemical

* Corresponding author.

and physical stability in aqueous systems, this oxide has also been investigated as a photocatalyst for water decontamination [8,9]. A particularly interesting case is the photochemical oxidative process, whereby the surface of a semiconductor is activated by UV radiation to generate free radicals for oxidation of organic compounds [9,10].

There is a continuous search for strategies to improve the photocatalytic activity of semiconductors and obtain these materials in immobilized form. Powder photocatalysts, although commonly used and advantageous in terms of surface area, are notoriously difficult to remove from the medium [11]. Furthermore, suspended particles tend to aggregate, which decreases their efficiency in new cycles, especially in reactions where the concentration of suspended particles is high. Suspensions cannot be reliably applied in continuous flow systems, as the photocatalyst is often lost [12,13]. In such a scenario, immobilization arises as a valuable technique that facilitates the use and reuse of semiconductor materials [14–17]. There are some reports of the synthesis of ZnO in immobilized form, with specific focus on thin films [18,19]. Jongnavakit et al. [18] obtained ZnO films immobilized on glass substrates by a sol–gel dip-coating technique. Lower withdrawal speeds resulted in ZnO films with a denser surface because of a decrease in particle size. This effect, in turn, reduced the distance between the solids under a water droplet, increasing the strength of pinning effects and the water contact angle. The improvement of crystallinity and surface roughness of ZnO thin films promoted by an increase in calcination temperature enhanced the photocatalytic activity of methylene blue degradation. Wanotayan et al. [19] synthesized nanostructured ZnO thin films by electrodeposition and subsequent heat treatment. Using annealing temperatures ranging from 300°C to 600°C, the authors developed films with varied microstructures and distinct properties. The photocatalytic activities of ZnO films were then studied in the photodegradation of methylene blue dye under UV light. The ZnO film fabricated at 500°C exhibited relatively high surface area, had the strongest photocatalytic activity, and showed good stability after successive reaction cycles.

ZnO films can be prepared by different techniques, which offers the possibility of selecting the most appropriate synthetic route according to the desired morphological characteristics [20]. Of note, the photocatalytic efficiency of semiconductor films is greatly dependent on factors such as crystal growth and orientation [15]. Compared with powder catalysts, film materials have easy separation and recovery [13]. Pal and Sharon [21] synthesized porous ZnO thin films by the sol–gel method using zinc acetate and found that the films had good catalytic efficiency in the decomposition of phenol, chlorophenol, naphthalene, and anthracene to CO_2. Kumar et al. [22] used ZnO thin films produced by co-sputtering to degrade 2-chlorophenol. Reusability assays showed that, after four cycles, ZnO thin films were still effective in catalyzing organic matter degradation, with no significant changes in photocatalytic efficiency. Sacco et al. [23] prepared a ZnO photocatalyst immobilized on commercial zeolite pellets (ZEO) by the wet impregnation method. ZnO/ZEO was applied for caffeine removal from aqueous solutions. The catalyst retained its oxidation efficiency after several reuse cycles.

Although the literature [24–26] on ZnO thin films is extensive, further research on deposition methods can contribute to improving their intrinsic properties. Additionally, it can help elucidate the relationship of structure and morphology with photocatalytic activity. Yang et al. [27] prepared ZnO thin films via the chemical bath deposition method without using any catalysts or templates. The effects of solvents (such as water, ethanol, and *n*-propanol) on structure and morphology of ZnO thin films were investigated. Thin films prepared in different solvents had different sizes and morphologies and different growth behaviors. ZnO thin films prepared in water showed superior photocatalytic activity in the degradation of Rhodamine B compared with other specimens. Mao et al. [28] obtained ZnO micro/nanostructures with different morphologies through a solvothermal process in the presence of surfactants. The morphology of as-synthesized ZnO samples included nanospheres, hexagonal disks, hexagonal bilayer disk-like structures, and 3D flower-like hierarchitectures depending on surfactant conditions.

The aim was to synthesize ZnO thin films by combining two chemical methods, polymeric precursor (PP) synthesis and microwave-assisted hydrothermal (HMW) synthesis. The advantages of the PP method include reasonable stoichiometric control and fine deposition of oxides [29]. HMW can achieve higher reaction rates in shorter times [30] and at lower temperatures than conventional heat-based methods. The central idea consists in harnessing the advantages of both methods to obtain ZnO thin films composed of two layers. This strategy is expected to produce ZnO thin films with excellent substrate adhesion properties, a greater number of active sites, improved photocatalytic activity, and enhanced stability in reuse cycles, representing a promising alternative to remove contaminants and reduce environmental pollution.

2. Materials and methods

2.1. Synthesis of ZnO thin films

2.1.1. PP method

ZnO was deposited on glass substrates by the PP method [31]. The reactants used were zinc acetate ($Zn(CH_3COO)_2$, Synth), citric acid ($C_6H_8O_7$, Synth), ethanol (CH_3CH_2OH, Synth), and ethylene glycol ($HOCH_2CH_2OH$, Synth). First, zinc acetate (10.0 g) was mixed with citric acid (26.0 g). The mixture was then added to 400 mL of ethanol under constant stirring at about 70°C. Nitric acid was added at this stage to promote the dissolution of precursors. At last, 16 mL of ethylene glycol was added for citrate polymerization. For synthesis by the PP method, the viscosity of the polymeric solution was adjusted to 12 mPa by modifying the water content. Viscosity analyses were performed on a Brookfield viscometer (ADV). Next, films were deposited onto glass substrates (1 cm × 1 cm) by the spin coating technique. A few drops of the polymeric solution were placed onto the substrate, which was then spun in a spin coater (1-EC101DT-R790, Headway Research, Inc.) at 6,000 rpm for 30 s. After each layer was deposited, the substrate was dried on a hot plate (~50°C) for a few seconds. A two-stage heat treatment was used. In the first stage, films were heated to 300°C at a heating rate of 1°C/min for 2 h to promote the

pyrolysis of organic material. In the second stage, films were heated to 450°C at 1°C/min, then cooled down at the same rate. Heat treatments were performed in an EDG-3000 furnace.

2.1.2. HMW method

The films obtained by the PP method as described in (Section 2.1.1 – PP method) were subjected to a subsequent deposition step by the HMW method, affording PP-HMW ZnO thin films. That is, PP films were used as a seed layer for HMW deposition. HMW synthesis of ZnO films was performed according to the procedures described by Wojnarowicz et al. [32]. Briefly, 1.66 g of zinc acetate, 25.00 mL of ethylene glycol, and 0.150 mL of deionized water were added to a beaker and maintained under magnetic stirring at 100 rpm and 70°C for 20 min. After this period, the solution was transferred to an Erlenmeyer flask containing ZnO films obtained by the PP method. The flask was sealed with a rubber stopper and treated in a microwave digestion system (MARS™ 6, CEM) at 600 W with a heating ramp of 5 min to 180°C. The plateau time varied from 10 min (PP-HMW-10) to 30 min (PP-HMW-30). Upon completion of the reaction, samples were subjected to heat treatment at 600°C for 2 h at a heating rate of 1°C/min.

2.2. Characterization

X-ray diffractometry (XRD) was used to examine film structural properties. Analyses were performed using a Bruker D8 Advance ECO X-ray diffractometer in the 2θ range of 20°–90° at a scanning rate of 4.5°/min. Film morphology was determined by field-emission scanning electron microscopy (FE-SEM), performed on a FEI Magellan 400 L apparatus. Bandgap values were determined by diffuse reflectance spectra (DRS) in the ultraviolet/visible/near-infrared (UV-Vis-NIR) region (200–1,200 nm) using a Shimadzu UV-Vis (Tokyo, Japan) equipment in the diffuse reflectance mode at room temperature. Bandgap energies were estimated by applying the Kubelka–Munk function [33,34] and constructing Tauc plots.

2.3. Photocatalytic assays

The photocatalytic activity of films was tested in the oxidation of Rhodamine B (RhB) under UV-C illumination. Films were repeatedly subjected to the same conditions to evaluate their potential for reuse over five photocatalytic cycles. First, photocatalysts were submerged in a 15 mL beaker containing RhB solution (5 mg/L) during 120 min. Assays were performed in a batch reactor equipped with four 15 W Philips mercury lamps (UV-C, λ = 254 nm). The reduction in dye concentration was estimated based on color removal percentage (%), which was determined by spectrophotometry (Cary 60 UV-Vis, Agilent Spectrophotometer, Santa Clara, CA, EUA, λ = 554 nm).

3. Results and discussion

3.1. Characterization

XRD was used to characterize ZnO films obtained by HMW treatment. As seen in the diffractogram of Fig. 1, HMW treatment promoted the formation of the typical wurtzite ZnO phase from the crystal plane in both PP-HMW-10 and PP-HMW-30, according to JCPDS file number 361451 [35]. Additionally, there was a decrease in the amorphous halo compared with the PP film. Heat-treated samples showed an increase in the intensity of crystal planes after exposure to microwave radiation for 10 or 30 min. This finding can be attributed to an increase in crystallinity and formation of the ZnO phase promoted by exposure to microwave energy, which enhanced network order.

Film crystallization quality was influenced by synthesis time in samples subjected to HMW treatment (Fig. 1). The diffractogram of films treated for the longest time (30 min) exhibits more well-defined peaks with higher intensity. Both PP-HMW films showed preferential orientation in the (002) plane. Amrani and Hamzaoui [36] obtained ZnO thin films deposited by sputtering and observed a preferential orientation in the (002) plane. The authors attributed these results to the reduced energy loss of atoms, which influences the growing film. Consequently, the collision frequency of atoms with plasma neutrals at low pressures is lower than at higher ones. Therefore, particles have more energy to rearrange themselves according to the hexagonal wurtzite crystal structure at the substrate surface. An important factor determining the preferred orientation of thin films is the relationship between minimum surface free energy and volume energy. The surface-to-volume ratio is high at a lower thickness, and more densely packed planes have lower surface free energy. For example, in ZnO films, the (002) plane has the most inferior surface free energy [37]. These mechanisms are governed by physical processes of deposition.

In chemical processes, the oriented growth of films can be related to the nature of the solvent and the ability to complex Zn(II). For example, Znaidi et al. [38] obtained ZnO thin films by the sol–gel method using two solvents, ethanol and 2-methoxy ethanol. Use of 2-methoxy ethanol promoted a well-defined orientation of the (002) plane. This preferential alignment was attributed to the boiling point and ability to

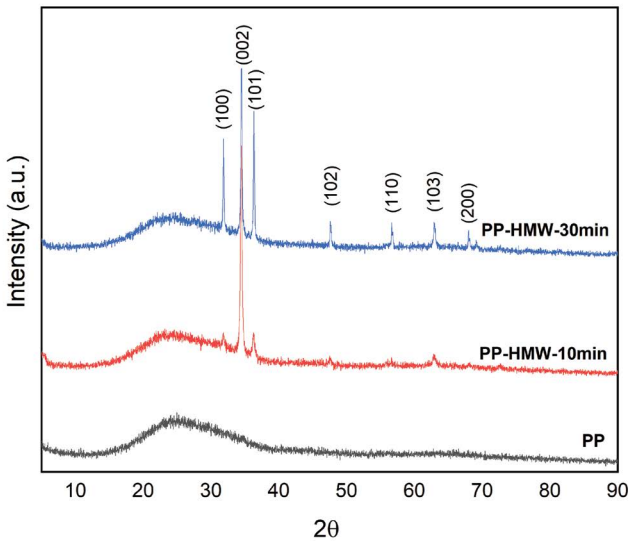

Fig. 1. X-ray diffractograms of ZnO films.

complex Zn(II). On the other hand, the initial Zn-oxo acetate gel can rearrange more completely in 2-methoxy ethanol. The solvent is more stable at relatively high temperatures during deposition–thermal treatment cycles (2-methoxy ethanol boiling point = 125°C) than ethanol (boiling point = 78°C). ZnO seeds exhibited agglomerated particles, which can contribute to defining orientation, as random nucleation is more probable in smaller-sized samples. In the present study, ZnO films were synthesized by HMW treatment using ethylene glycol as solvent. It is believed that the preferred orientation observed in the (002) plane was promoted by the high boiling point of ethylene glycol (197°C) and the solvent's ability to complex Zn(II), as previously discussed.

Fig. 2 shows the scanning electron microscopy (SEM) images of PP, PP-HMW-10, and PP-HMW-30 ZnO thin films. All samples displayed smooth, crack-free surfaces, indicating oxide phase formation, such as organics, and elimination of intermediates during heat treatment. The homogeneity of the film–substrate interface observed in all samples suggests good film adhesion. Such good adhesion is due to the ZnO seed layer (Fig. 2a), as confirmed by SEM with energy-dispersive X-ray spectroscopy (EDX) (Fig. 3). SEM-EDX analysis of the ZnO film obtained by PP deposition showed a homogeneous surface, suitable as a base layer for future processing steps. The presence of Zn and O elements was observed along the entire surface of the film, indicating material homogeneity.

Elemental composition analysis revealed the presence of Zn and O in greater intensity, corroborating ZnO detection. Si, Al, and Mg, which compose the support glass, were detected at lower concentrations. C is attributed to the carbon tape that supports the film, as depicted in SEM images. The findings show that the precursor film exhibited homogeneity and elemental purity before microwave processing and heat treatment.

Fig. 2b shows the SEM images of PP-HMW-10. A first layer with a stable surface and nanometric dimensions (32 nm) was identified. The surface of this layer contained agglomerates ranging from 330 nm to 1.213 μm in diameter. Agglomerates were composed of particles measuring 30–117 nm in diameter. Thus, it appears that HMW treatment leads to the formation of a homogeneous layer with complete saturation until the following layer is formed. PP-HMW-30 exhibited a surface filled with superimposed agglomerates ranging from 252 nm to 1.164 μm in diameter, composed of 25–137 nm particles (Fig. 2c). Thus, the addition of the HMW stage, conducted in an aqueous medium under high pressure and temperature conditions, allows for simultaneous occurrence of dissolution and precipitation. Consequently, the process is favorable to particle changes, as verified by the decrease in particle size of thin films treated for 30 min (PP-HMW-30).

UV-Vis spectroscopy was used to assess the optical properties of ZnO films. Fig. 4 shows the Tauc plots [39] used to determine the direct optical gap (n = 1/2) from the intercept

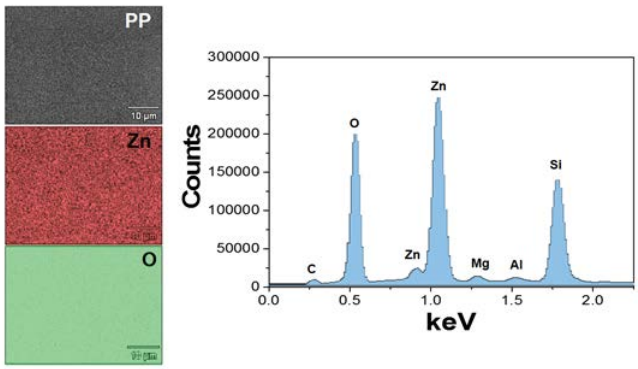

Fig. 3. Energy-dispersive X-ray spectra of PP film.

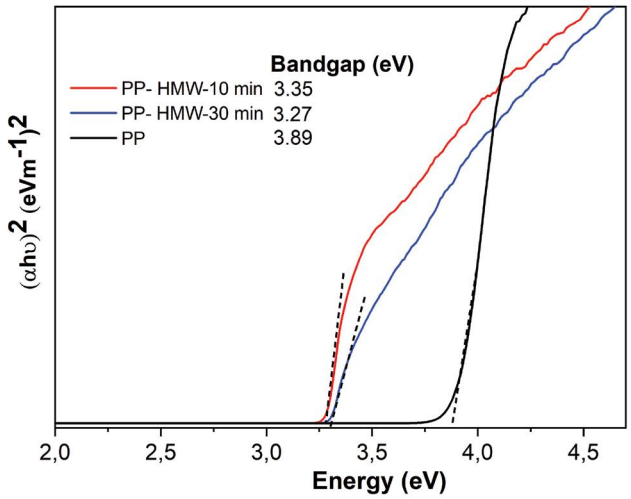

Fig. 4. Tauc's plots of ZnO films.

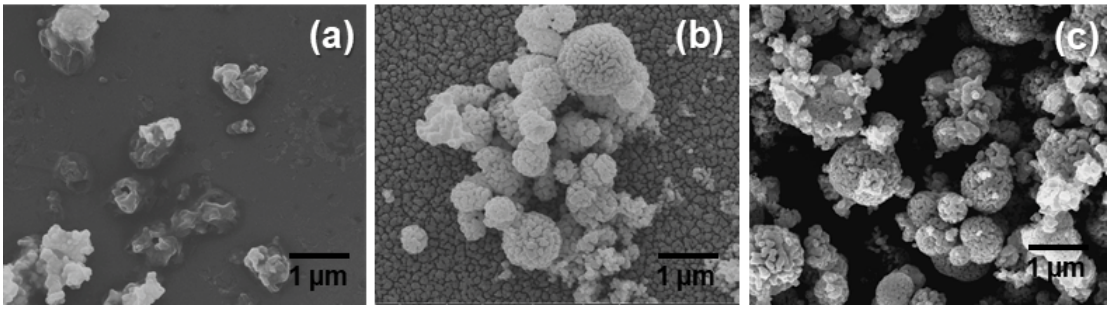

Fig. 2. Scanning electron microscopy-field emission gun micrographs of ZnO films. (a) PP, (b) PP-HMW-10 min and (c) PP-HMW-30 min.

of ($\alpha h\nu$)2 vs. $h\nu$. For all PP-HMW samples, the direct gap energy value was about 3.3 eV. The values found here for bandgap energy are consistent with those reported in the literature for ZnO [40,41]. However, the PP thin film had a greater bandgap energy (3.9 eV) than PP-HMW films. This result can be explained by the fact that the PP film has a more homogeneous surface and lower ZnO typical structural phase (Fig. 1). As a result, it undergoes less deformation than PP-HMW films and, consequently, has higher bandgap values [42].

3.2. Photocatalytic assays

Dye degradation assays were carried out to assess the oxidative potential of samples. Synthesized films were used to oxidize an RhB solution under UV irradiation. Fig. 5 shows the color removal profiles of RhB in the presence of ZnO films under UV irradiation. A similar experiment was performed in the dark to assess RhB adsorption, and no color removal was observed after 120 min, indicating that adsorption does not occur under these conditions.

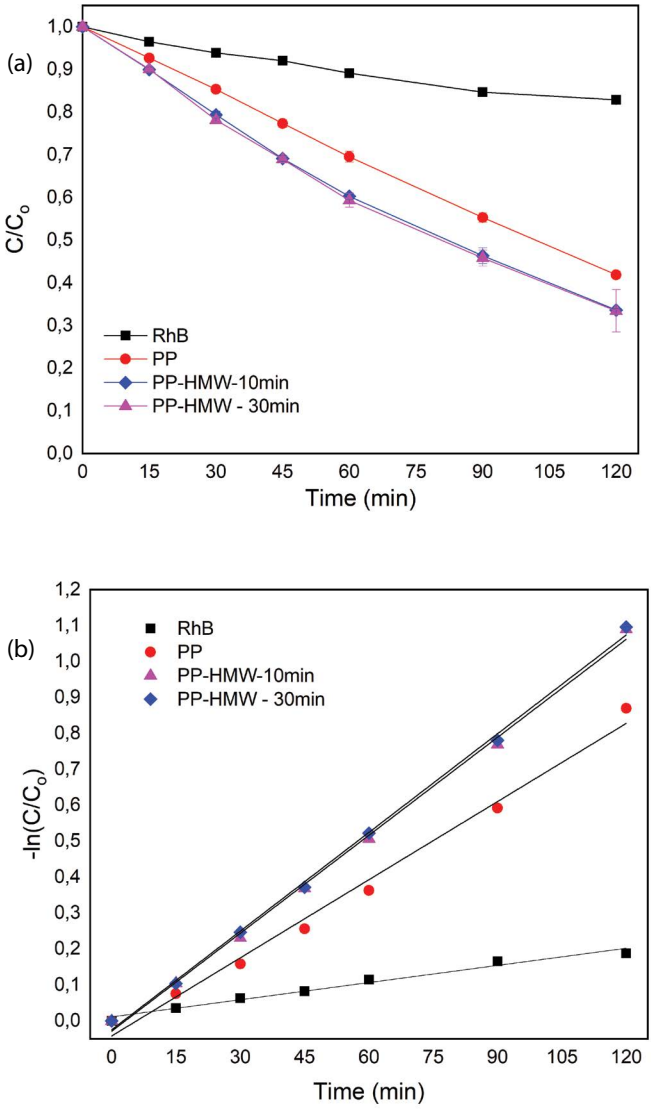

Fig. 5. Kinetic study for photocatalytic degradation of Rhodamine B dye: (a) color remotion according to the time of process and (b) first-order kinetics of degradation by employing the ZnO films.

Fig. 6 shows a cross-sectional view of the PP-HMW-10 film. The difference between the seed layer and agglomerates from HMW deposition is clear. ZnO films obtained using PP-HMW exhibited the same photocatalytic activity, promoting 67% RhB degradation in 120 min. This result indicates that HMW synthesis time did not influence the photocatalytic properties of materials. Furthermore, PP-HMW films had better photocatalytic activity than the PP film, which reached 58% degradation. These results show that combining synthetic methods improved the photocatalytic activity of ZnO thin films. Photoactivity gain is attributed to the interface formation, which generates a rough film, enhancing contact between RhB dye and the semiconductor. Photocatalysis occurs at the interface between the catalyst and organic pollutants [43]. It is well known that photocatalytic activity is closely related to catalyst surface area, in that large surface areas imply more active sites [44–47]. Therefore, rough structures may effectively improve the photocatalytic activity of semiconductor materials.

Dye decolorization was monitored over time, allowing the reaction rate constant to be calculated. Eq. (1) relates the degradation time to RhB concentration:

$$-\ln\left(\frac{\mathrm{RhB}}{\mathrm{RhB}_0}\right) = -\ln\left(\frac{C}{C_0}\right) = k't \tag{1}$$

where $k' = k$ [AS], k is the reaction rate constant (min^{-1}), [AS] is the concentration of active sites on the photocatalyst surface, t (min) is the irradiation time, and C is the RhB concentration (mg/L) [48].

The formation of radicals responsible for dye degradation is correlated to high-rate constants (k'). However,

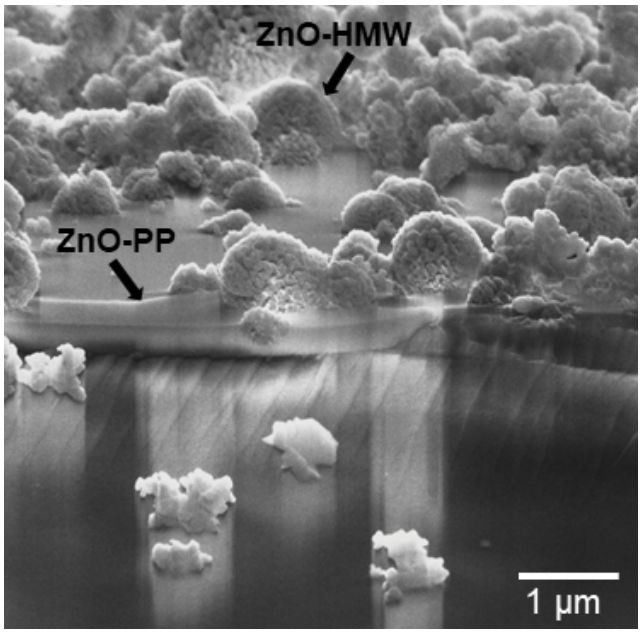

Fig. 6. Cross-section of the PP-HMW-10 film.

Table 1
First kinetic values of k', $t_{1/2}$ and R^2 for each sample and blank (RhB)

Parameters	Rhodamine B	PP	PP-HMW-10 min	PP-HMW-30 min
k' (10^{-3} min^{-1})	1.59	7.25	9.09	9.15
R^2	0.98	0.99	0.99	0.99
$t_{1/2}$	435.8	95.6	76.2	75.7

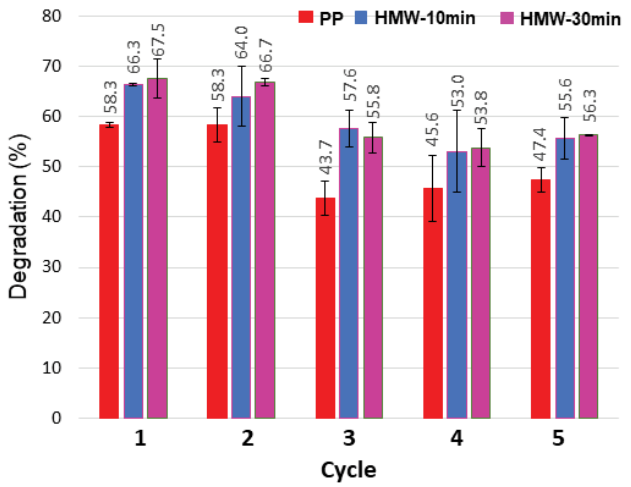

Fig. 7. Rhodamine B photocatalytic degradation cycles of ZnO films.

for k' to be high, the concentration of available active sites must also be increased. Therefore, the number of active sites will strongly influence degradation kinetics, given that these parameters are directly proportional, as depicted in Eq. (1). According to Eq. (1), $-\ln(C/C_0)$ vs. t represents a curve with an angular coefficient equal to k'. Fig. 4b depicts the graph of $-\ln(C/C_0)$ vs. t. All reactions were found to follow first-order kinetics, indicating that all degradation reactions have the same mechanism.

Eq. (2) was used to estimate the time required to reduce the concentration of organic compounds by half:

$$t_{1/2} = \frac{\ln 2}{k'} \tag{2}$$

where $t_{1/2}$ (min) is the half-life.

Table 1 lists the k' values obtained from Fig. 4b and the respective half-life values, calculated from Eqs. (1) and (2), respectively.

These results are associated with the surface characteristics of materials. For example, PP films have a homogeneous layer free of pores. In addition, HMW treatment, which resulted in heterogeneous agglomerates and reduced particle size, promoted an increase in the diffusional exchange of molecules from the aqueous medium to the film surface, increasing efficiency.

Film reusability is an essential parameter for practical application. The reusability of samples was analyzed for up to five cycles. After each cycle, thin films were subjected to heat treatment at 300°C to remove RhB residues. As shown in Fig. 7, PP-HMW films exhibited the highest reuse capacity (67.5% in the first cycle and 56.3% in the last cycle) compared with the PP film (58.3% in the first cycle and 47.4% in the last cycle). These results corroborate that PP-HMW films have superior performance to PP films. Photocatalytic activity was not influenced by synthesis time. After the second cycle, there was a slight decrease in photocatalytic activity in all films. Nevertheless, all samples showed good photocatalytic activity and a high potential for reuse. The findings revealed that ZnO thin films are stable and retain their photocatalytic activity in aqueous media during subsequent reuse cycles.

4. Conclusion

This paper reported the successful preparation of ZnO films through a combination of chemical methods, namely PP synthesis and HMW treatment. A second layer of ZnO (PP-HMW) was deposited on the seed layer (PP method), promoting modification of structural and morphological properties of thin films. All ZnO thin films exhibited a pure wurtzite phase. However, PP-HMW films showed a preferential orientation in the (002) plane. PP-HMW films exhibited a minor bandgap energy of 3.3 eV rather than 3.9 eV (PP film). PP-HMW film surface contained large particle agglomerates, resulting in an uneven, rough texture. As a result, the efficiency of PP-HMW films was higher than that of the PP film. PP-HMW films obtained in 10 and 30 min of synthesis showed similar photocatalytic efficiencies (67%) in RhB degradation. Thus, synthesis time did not influence the photocatalytic properties of films. Such results can be attributed to the interface between PP and HMW layers, which increased surface irregularity and enhanced contact between pollutant and semiconductor. Photocatalysts maintained integrity after five use cycles (56% dye removal). The combination of PP and HMW treatment led to improvements in the photocatalytic properties of ZnO thin films, indicating potential for environmental remediation.

Acknowledgements

The authors thank CNPq and FAPEMIG for the financial support. They also thank the Laboratory of Structural Characterization (LCE/DEMa/UFSCar) for providing general facilities. The authors acknowledge SisNano/MCTIC, EMBRAPA, and CAPES.

Funding

This study was supported by the Brazilian Federal Agency for Support and Evaluation of Graduate Education (CAPES, Finance Code 001).

Conflicts of interest/competing interests

The authors declare that they have no conflict of interest.

Data availability

The authors declare that all data supporting the findings of this study are available within the article and its supplementary information files.

References

[1] M. Rincón Joya, J. Barba Ortega, J.O.D. Malafatti, E.C. Paris, Evaluation of photocatalytic activity in water pollutants and cytotoxic response of α-Fe_2O_3 nanoparticles, ACS Omega, 4 (2019) 17477–17486.

[2] A.M. Raba-Páez, J.O.D. Malafatti, C.A. Parra-Vargas, E.C. Paris, M. Rincón-Joya, Structural evolution, optical properties, and photocatalytic performance of copper and tungsten heterostructure materials, Mater. Today Commun., 26 (2021) 101886, doi: 10.1016/j.mtcomm.2020.101886.

[3] S. Agarwal, S. Kumar, H. Agrawal, M.G. Moinuddin, M. Kumar, S.K. Sharma, K. Awasthi, An efficient hydrogen gas sensor based on hierarchical Ag/ZnO hollow microstructures, Sens. Actuators, B, 346 (2021) 130510, doi: 10.1016/j.snb.2021.130510.

[4] T. Tian, L. Zheng, M. Podlogar, H. Zeng, S. Bernik, K. Xu, X. Ruan, X. Shi, G. Li, Novel ultrahigh-performance ZnO-based varistor ceramics, ACS Appl. Mater. Interfaces, 13 (2021) 35924–35929.

[5] S. da C. Brito, J.O.D. Malafatti, F.E. Arab, J.D. Bresolin, E.C. Paris, C.W.O. de Souza, M.D. Ferreira, One-pot synthesis of CuO, ZnO, and Ag nanoparticles: structural, morphological, and bactericidal evaluation, Inorg. Nano-Metal Chem., 53 (2023) 490–500.

[6] L.G.S. Peres, J.O.D. Malafatti, B. Bernardi, L.H.C. Mattoso, E.C. Paris, Biodegradable starch sachets reinforced with montmorillonite for packing ZnO nanoparticles: solubility and Zn^{2+} ions release, J. Polym. Environ., 31 (2023) 2388–2398.

[7] C. El Bekkali, H. Bouyarmane, M. El Karbane, S. Masse, A. Saoiabi, T. Coradin, A. Laghzizil, Zinc oxide-hydroxyapatite nanocomposite photocatalysts for the degradation of ciprofloxacin and ofloxacin antibiotics, Colloids Surf., A, 539 (2018) 364–370.

[8] P. Pascariu, L. Olaru, A.L. Matricala, N. Olaru, Photocatalytic activity of ZnO nanostructures grown on electrospun CAB ultrafine fibers, Appl. Surf. Sci., 455 (2018) 61–69.

[9] M. Sharma, A. Kumar, R.K. Gautam, M. Belwal, Synthesis and characterization of ZnO-CeO_2 nanocomposite with enhanced UV-light-driven photocatalytic dye degradation of Rhodamine-B, J. Nanosci. Nanotechnol., 18 (2017) 3532–3535.

[10] A.J. Moreira, J.O.D. Malafatti, T.R. Giraldi, E.C. Paris, E.C. Pereira, V.R. de Mendonça, V.R. Mastelaro, G.P.G. Freschi, Prozac® photodegradation mediated by Mn-doped TiO_2 nanoparticles: evaluation of by-products and mechanisms proposal, J. Environ. Chem. Eng., 8 (2020) 104543, doi: 10.1016/j.jece.2020.104543.

[11] E.C. Paris, J.O.D. Malafatti, C.R. Sciena, L.F. Neves Junior, A. Zenatti, M.T. Escote, A.J. Moreira, G.P.G. Freschi, Nb_2O_5 nanoparticles decorated with magnetic ferrites for wastewater photocatalytic remediation, Environ. Sci. Pollut. Res., 28 (2021) 23731–23741.

[12] I.M. Arabatzis, S. Antonaraki, T. Stergiopoulos, A. Hiskia, E. Papaconstantinou, M.C. Bernard, P. Falaras, Preparation, characterization and photocatalytic activity of nanocrystalline thin film TiO_2 catalysts towards 3,5-dichlorophenol degradation, J. Photochem. Photobiol., A, 149 (2002) 237–245.

[13] S. Ayyaru, T.T.L. Dinh, Y.-H. Ahn, Enhanced antifouling performance of PVDF ultrafiltration membrane by blending zinc oxide with support of graphene oxide nanoparticle, Chemosphere, 241 (2020) 125068, doi: 10.1016/j.chemosphere.2019.125068.

[14] F. Gallino, C. Di Valentin, G. Pacchioni, M. Chiesa, E. Giamello, Nitrogen impurity states in polycrystalline ZnO. A combined EPR and theoretical study, J. Mater. Chem., 20 (2010) 689–697.

[15] K.M. Lee, C.W. Lai, K.S. Ngai, J.C. Juan, Recent developments of zinc oxide based photocatalyst in water treatment technology: a review, Water Res., 88 (2016) 428–448.

[16] E.C. Paris, J.O.D. Malafatti, A.J. Moreira, L.C. Santos, C.R. Sciena, A. Zenatti, M.T. Escote, V.R. Mastelaro, M.R. Joya, CuO nanoparticles decorated on hydroxyapatite/ferrite magnetic support: photocatalysis, cytotoxicity, and antimicrobial response, Environ. Sci. Pollut. Res., 29 (2022) 41505–41519.

[17] A.M. Raba-Páez, J.O.D. Malafatti, C.A. Parra-Vargas, E.C. Paris, M. Rincón-Joya, Effect of tungsten doping on the structural, morphological and bactericidal properties of nanostructured CuO, PLoS One, 15 (2020) 1–16.

[18] P. Jongnavakit, P. Amornpitoksuk, S. Suwanboon, T. Ratana, Surface and photocatalytic properties of ZnO thin film prepared by sol–gel method, Thin Solid Films, 520 (2012) 5561–5567.

[19] T. Wanotayan, J. Panpranot, J. Qin, Y. Boonyongmaneerat, Microstructures and photocatalytic properties of ZnO films fabricated by Zn electrodeposition and heat treatment, Mater. Sci. Semicond. Process., 74 (2018) 232–237.

[20] V.K. Jayaraman, A. Hernández-Gordillo, M. Bizarro, Importance of precursor type in fabricating ZnO thin films for photocatalytic applications, Mater. Sci. Semicond. Process., 75 (2018) 36–42.

[21] B. Pal, M. Sharon, Enhanced photocatalytic activity of highly porous ZnO thin films prepared by sol–gel process, Mater. Chem. Phys., 76 (2002) 82–87.

[22] R. Kumar, M.S. Abdel-Wahab, M.A. Barakat, J. Rashid, N. Salah, A.A. Al-Ghamdi, Role of N doping on the structural, optical and photocatalytic properties of the silver deposited ZnO thin films, J. Taiwan Inst. Chem. Eng., 69 (2016) 131–138.

[23] O. Sacco, V. Vaiano, M. Matarangolo, ZnO supported on zeolite pellets as efficient catalytic system for the removal of caffeine by adsorption and photocatalysis, Sep. Purif. Technol., 193 (2018) 303–310.

[24] M.R. Islam, M. Rahman, S.F.U. Farhad, J. Podder, Structural, optical and photocatalysis properties of sol–gel deposited Al-doped ZnO thin films, Surf. Interfaces, 16 (2019) 120–126.

[25] J.K. Saha, R.N. Bukke, N.N. Mude, J. Jang, Significant improvement of spray pyrolyzed ZnO thin film by precursor optimization for high mobility thin film transistors, Sci. Rep., 10 (2020) 1–11.

[26] P.C. Lee, Y.L. Hsiao, J. Dutta, R.C. Wang, S.W. Tseng, C.P. Liu, Development of porous ZnO thin films for enhancing piezoelectric nanogenerators and force sensors, Nano Energy, 82 (2021) 105702, doi: 10.1016/j.nanoen.2020.105702.

[27] J. Yang, B. Wei, X. Li, J. Wang, H. Zhai, X. Li, Y. Sui, Y. Liu, J. Wang, J. Lang, Q. Zhang, Synthesis of ZnO films in different solvents and their photocatalytic activities, Cryst. Res. Technol., 50 (2015) 840–845.

[28] Y. Mao, Y. Li, Y. Zou, X. Shen, L. Zhu, G. Liao, Solvothermal synthesis and photocatalytic properties of ZnO micro/nanostructures, Ceram. Int., 45 (2019) 1724–1729.

[29] J.A. Oliveira, A.E. Nogueira, M.C.P. Gonçalves, E.C. Paris, C. Ribeiro, G.Y. Poirier, T.R. Giraldi, Photoactivity of N-doped ZnO nanoparticles in oxidative and reductive reactions, Appl. Surf. Sci., 433 (2018) 879–886.

[30] J. Huang, C. Xia, L. Cao, X. Zeng, Facile microwave hydrothermal synthesis of zinc oxide one-dimensional nanostructure with three-dimensional morphology, Mater. Sci. Eng., B, 150 (2008) 187–193.

[31] U. Choppali, E. Kougianos, S.P. Mohanty, B.P. Gorman, Influence of annealing on polymeric precursor derived ZnO thin films on sapphire, Thin Solid Films, 545 (2013) 466–470.

[32] J. Wojnarowicz, T. Chudoba, S. Gierlotka, K. Sobczak, W. Lojkowski, Size control of cobalt-doped zno nanoparticles obtained in microwave solvothermal synthesis, Crystals, 8 (2018) 1–18.

[33] C. Sandoval, A.D. Kim, Deriving Kubelka–Munk theory from radiative transport, J. Opt. Soc. Am. A, 31 (2014) 628, doi: 10.1364/josaa.31.000628.

[34] O. Schevciw, W.B. White, The optical absorption edge of rare earth sesquisulfides and alkaline earth – rare earth sulfides, Mater. Res. Bull., 18 (1983) 1059–1068.
[35] A. Dhanalakshmi, A. Palanimurugan, B. Natarajan, Efficacy of saccharides bio-template on structural, morphological, optical and antibacterial property of ZnO nanoparticles, Mater. Sci. Eng., C, 90 (2018) 95–103.
[36] B. Amrani, S. Hamzaoui, Characterization of ZnO films prepared by reactive sputtering at different oxygen pressures, Catal. Today, 89 (2004) 331–335.
[37] K.C. Sanal, R.R. Trujillo, P.K. Nair, M.T.S. Nair, Room Temperature Deposition of Zinc Oxide Thin Films by RF-Magnetron Sputtering for Application in Solar Cells, SPIE Optics + Photonics for Sustainable Energy, 2016. https://doi.org/10.1117/12.2238434.
[38] L. Znaidi, G.J.A.A. Soler Illia, R. Le Guennic, C. Sanchez, A. Kanaev, Elaboration of ZnO thin films with preferential orientation by a soft chemistry route, J. Sol-Gel Sci. Technol., 26 (2003) 817–821.
[39] J. Zhang, P. Zhou, J. Liu, J. Yu, New understanding of the difference of photocatalytic activity among anatase, rutile and brookite TiO_2, Phys. Chem. Chem. Phys., 16 (2014) 20382–20386.
[40] M. Kahouli, A. Barhoumi, A. Bouzid, A. Al-Hajry, S. Guermazi, Structural and optical properties of ZnO nanoparticles prepared by direct precipitation method, Superlattices Microstruct., 85 (2015) 7–23.
[41] A. Sáenz-Trevizo, P. Amézaga-Madrid, P. Pizá-Ruiz, W. Antúnez-Flores, M. Miki-Yoshida, Optical bandgap estimation of ZnO nanorods, Mater. Res., 19 (2016) 33–38.
[42] A.K. Jazmati, B. Abdallah, Optical and structural study of ZnO thin films deposited by RF magnetron sputtering at different thicknesses: a comparison with single crystal, Mater. Res., 21 (2018) 20170821, doi: 10.1590/1980-5373-MR-2017-0821.
[43] J.O.D. Malafatti, A.J. Moreira, C.R. Sciena, T.E.M. Silva, G.P.G. Freschic, E.C. Pereira, E.C. Paris, Prozac® removal promoted by HAP:Nb_2O_5 nanoparticles system: by-products, mechanism, and cytotoxicity assessment, J. Environ. Chem. Eng., 9 (2021) 104820, doi: 10.1016/j.jece.2020.104820.
[44] H. Fu, J. Lin, L. Zhang, Y. Zhu, Photocatalytic activities of a novel $ZnWO_4$ catalyst prepared by a hydrothermal process, Appl. Catal., A, 306 (2006) 58–67.
[45] X.C. Song, Y.F. Zheng, R. Ma, Y.Y. Zhang, H.Y. Yin, Photocatalytic activities of Mo-doped Bi_2WO_6 three-dimensional hierarchical microspheres, J. Hazard. Mater., 192 (2011) 186–191.
[46] Y. Tong, J. Cheng, Y. Liu, G.G. Siu, Enhanced photocatalytic performance of ZnO hierarchical nanostructures synthesized via a two-temperature aqueous solution route, Scr. Mater., 60 (2009) 1093–1096.
[47] X. Xu, X. Duan, Z. Yi, Z. Zhou, X. Fan, Y. Wang, Photocatalytic production of superoxide ion in the aqueous suspensions of two kinds of ZnO under simulated solar light, Catal. Commun., 12 (2010) 169–172.
[48] V.R. De Mendonça, C. Ribeiro, Influence of TiO_2 morphological parameters in dye photodegradation: a comparative study in peroxo-based synthesis, Appl. Catal., B, 105 (2011) 298–305.